PLOS ONE

RESEARCH ARTICLE

Anti-inflammatory effects of cold atmospheric plasma irradiation on the THP-1 human acute monocytic leukemia cell line

Ito Hirasawa[1,2], Haruka Odagiri[2], Giri Park[2], Rutvi Sanghavi[2], Takaya Oshita[2], Akiko Togi[2†], Katsunori Yoshikawa[2]*, Koji Mizutani[1], Yasuo Takeuchi[3], Hiroaki Kobayashi[1], Sayaka Katagiri[1], Takanori Iwata[1], Akira Aoki[1]*

1 Department of Periodontology, Graduate School of Medical and Dental Sciences, Tokyo Medical and Dental University, Tokyo, Japan, 2 Sekisui Chemical Co., Ltd., Ibaraki, Japan, 3 Department of Lifetime Oral Health Care Science, Graduate School of Medical and Dental Sciences, Tokyo Medical and Dental University, Tokyo, Japan

† Deceased.
* katsunori.yoshikawa@sekisui.com (KY); aoperi@tmd.ac.jp (AA)

Abstract

Cold atmospheric plasma (CAP) has been studied and clinically applied to treat chronic wounds, cancer, periodontitis, and other diseases. CAP exerts cytotoxic, bactericidal, cell-proliferative, and anti-inflammatory effects on living tissues by generating reactive species. Therefore, CAP holds promise as a treatment for diseases involving chronic inflammation and bacterial infections. However, the cellular mechanisms underlying these anti-inflammatory effects of CAP are still unclear. Thus, this study aimed to elucidate the anti-inflammatory mechanisms of CAP *in vitro*. The human acute monocytic leukemia cell line, THP-1, was stimulated with lipopolysaccharide and irradiated with CAP, and the cytotoxic effects of CAP were evaluated. Time-course differentiation of gene expression was analyzed, and key transcription factors were identified via transcriptome analysis. Additionally, the nuclear localization of the CAP-induced transcription factor was examined using western blotting. The results indicated that CAP showed no cytotoxic effects after less than 70 s of irradiation and significantly inhibited interleukin 6 (*IL6*) expression after more than 40 s of irradiation. Transcriptome analysis revealed many differentially expressed genes (DEGs) following CAP irradiation at all time points. Cluster analysis classified the DEGs into four distinct groups, each with time-dependent characteristics. Gene ontology and gene set enrichment analyses revealed CAP-induced suppression of *IL6* production, other inflammatory responses, and the expression of genes related to major histocompatibility complex (MHC) class II. Transcription factor analysis suggested that nuclear factor erythroid 2-related factor 2 (NRF2), which suppresses intracellular oxidative stress, is the most activated transcription factor. Contrarily, regulatory factor X5, which regulates MHC class II expression, is the most suppressed transcription factor. Western blotting revealed the nuclear localization of NRF2 following CAP irradiation. These data suggest that CAP suppresses the inflammatory response, possibly by promoting NRF2 nuclear translocation.

Introduction

Physical plasmas, recognized as the fourth state of matter, encompass excited ionized gases that comprise reactive species, atoms, electrons, and other constituents [1]. Recent technological advancements have facilitated the generation of physical plasma at low temperatures and under atmospheric pressure. This variant is commonly referred to as cold atmospheric plasma (CAP). By subjecting biological systems to CAP irradiation, a range of effects, such as cell proliferation, programmed cell death, anti-inflammatory responses, and sterilization, can be induced, primarily through the action of reactive oxygen and nitrogen species (RONS). The potential applications of CAP in diverse medical domains, including wound healing and cancer treatment, have been the subject of extensive investigation [1–3].

Periodontal disease is chronic periodontal tissue inflammation caused by microbiological dysbiosis involving gingival bleeding and loss of alveolar bone [4], and using CAP to treat periodontal diseases is also under consideration. CAP irradiation reportedly suppresses inflammatory cytokines and loss of alveolar bone in rat periodontitis [5], reduces periodontal pathogens, and improves bleeding on probing and the gingival index in a clinical study [6]. The bactericidal and anti-inflammatory effects are presumed to be the mechanisms underlying the improvement of periodontal disease induced by CAP.

RONS produced during CAP treatment destabilize bacterial structures, such as proteins, cellular envelopes, and DNA. This mechanism is widely acknowledged as the primary means by which CAP achieves sterilization [7,8]. However, the cellular mechanism of the anti-inflammatory effects of CAP remains unclear because of its varying effects from pro-inflammatory to anti-inflammatory, depending on the plasma dose and therapeutic target. CAP can suppress inflammation in monocytes [9], *ex vivo* human oral tissue [10], and periodontitis in a rat model [5]. In contrast, it promotes inflammation in keratinocytes [11], dendritic cells [12], and wound healing in a mouse model [13].

The nuclear factor erythroid 2-related factor 2 (NRF2) plays a crucial role in cellular reactions to plasma irradiation. NRF2 is a transcription factor (TF) that exerts cellular protective effects against oxidative stress via expressing antioxidant response element (ARE)-regulated genes. Microarray and proteomic analyses of CAP-treated keratinocytes have suggested NRF2 pathway activation [14]. Furthermore, histological and gene expression analyses confirmed the nuclear migration of NRF2 and ARE-regulated gene activation in a mouse wound model [13]. While the involvement of NRF2 in the plasma effect has been established in certain cell types, its contribution to the anti-inflammatory properties of CAP against immune cells during inflammatory conditions remains unclear. Furthermore, other TFs supporting the widespread activity of CAP have not yet been identified.

Therefore, we aimed to reveal the mechanism underlying the anti-inflammatory effects of CAP on the human acute monocytic leukemia cell line, THP-1, using transcriptome analysis.

Materials and methods

Cell culture and lipopolysaccharide (LPS) stimulation

The THP-1 cells (JCRB0112.1 / LOT:11012017, JCRB cell bank, Osaka, Japan) were cultured at 2×10^4 cells per well in a 96-well plate containing 100 µL RPMI 1640 (Fujifilm Wako Pure Chemical Corporation, Osaka, Japan) supplemented with 10% fetal bovine serum (FBS, Thermo Fisher Scientific, Waltham, MA, USA) and 1% penicillin-streptomycin (Fujifilm Wako Pure Chemical Corporation). The cells were incubated at 37°C in a humidified atmosphere containing 5% CO_2. Cells were stimulated with LPS from *Porphyromonas gingivalis*

(Pg, InvivoGen, San Diego, CA, USA) at a final concentration of 1 μg/mL or without LPS for 3 h in an FBS supplemented-culture medium.

CAP treatment

A CAP apparatus (Pidi™, Sekisui Chemical, Osaka, Japan) was used with nitrogen as the feed gas. THP-1 cells stimulated with LPS were treated with CAP for 70 s at a flow rate of 1 L/min, 12 mm from the bottom of the well. After plasma irradiation, cells were incubated at 37°C in 5% CO_2.

RONS measurements

Hydrogen peroxide (H_2O_2) and nitrite (NO_2^-) concentrations were measured in the medium with or without cells following the CAP irradiation using the Amplite™ Colorimetric Hydrogen Peroxide Assay Kit (AAT Bioquest, Pleasanton, CA, USA) and the NO_2/NO_3 Assay Kit-FX (Fluorometric) 2,3-Diaminonaphthalene Kit (Dojindo, Tokyo, Japan), respectively. Absorbance and fluorescence were measured using the Varioskan LUX (Thermo Fisher Scientific).

Cell viability assay

For CAP cytotoxicity evaluation, a 3-(4,5-dimethythizol-2-yl)-5-(3-carboxymethoxyphenyl)-2-(4-sulfophenyl)-2H-tetrazolium salt (MTS) assay and acridine orange (AO)/propidium iodide (PI) staining were conducted using the CellTiter 96® AQueous One Solution Cell Proliferation Assay (Promega, Madison, WI, USA) and the Cyto3D Live-Dead Assay Kit (TheWell Bioscience, North Brunswick Township, NJ, USA), respectively. After CAP irradiation, MTS or AO/PI reagent was added to the wells, and absorbance or fluorescence was measured using the Varioskan LUX (Thermo Fisher Scientific).

Reverse-transcription quantitative polymerase chain reaction (RT-qPCR)

RT-qPCR was performed to monitor Interleukin 6 (*IL6*) expression. After CAP irradiation, RNA was extracted from THP-1 cells and reverse-transcribed to synthesize cDNA using the CellAmp™ Direct RNA Prep Kit for RT-PCR (Takara Bio, Shiga, Japan). The PCR mixture was prepared using TB Green® Fast qPCR Mix (Takara Bio), and RT-qPCR was performed using the QuantStudio® 3 Real-Time PCR System (Thermo Fisher Scientific). Relative gene expression levels were calculated using the $2^{-\Delta\Delta CT}$ method [15], and glyceraldehyde-3-phosphate dehydrogenase (GAPDH) was used as the internal control. The PCR primers used in this study are listed in Table 1.

Enzyme-linked immunosorbent assay (ELISA)

Supernatants from LPS-stimulated THP-1 cell cultures were collected 12 and 24 h after CAP irradiation. IL6 in the medium was measured using an ELISA kit (R&D Systems, Minneapolis, MN, USA) according to the manufacturer's instructions.

Table 1. Primer sequences for RT-qPCR.

Target		sequence 5′→3′
GAPDH	forward	CATCTTCTTTTGCGTCGCC
	reverse	GTTAAAAGCAGCCCTGGTGAC
IL6	forward	GCTGATGGCCCTAAACAGA
	reverse	GGTGGTCGGAGATTCGTAG

https://doi.org/10.1371/journal.pone.0292267.t001

RNA extraction and RNA-Seq

Total RNA was extracted from LPS-stimulated THP-1 cells using the RNeasy Plus Mini Kit (QIAGEN, Netherlands) 3, 6, 12, 18, and 24 h after 0 or 70 s of CAP irradiation. THP-1 cells irradiated and non-irradiated with CAP were named as CAP-treated and non-treated, respectively. RNA-Seq libraries were prepared using the poly(A) enrichment technique using the SMART Seq® v4 Ultra® Low Input RNA Kit for sequencing (Clontech, Shiga, Japan) from the total RNA. The libraries were sequenced with 2× 150-bp pair-end reads on a NovaSeq 6000 system (Illumina, San Diego, CA, USA). RNA-Seq data obtained in this study are available from the DNA Data Bank of Japan (DDBJ; http://www.ddbj.nig.ac.jp/) under the accession number DRA016810. DRAGEN Bio-IT Platform v3.6.3 (Illumina, USA) was used to map the obtained RNA-Seq data to the human reference genome (GRCh38.primary_assembly. genome.fa.gz) and calculate the gene expression levels. Genes were annotated using the GEN-CODE annotation file (gencode.v35.primary_assembly.annotation.gtf.gz).

Western blotting

Nuclear proteins were extracted from THP-1 cells 3 h after CAP irradiation using the Nuclear Extraction Kit (Cayman Chemical, Ann Arbor, MI, USA). Protein samples were denatured with the 10× Bolt™ Sample Reducing Agent (Thermo Fisher Scientific) and the 4× Bolt™ LDS Sample Buffer (Thermo Fisher Scientific) separated by a Bolt™ 4 to 12% Bis-Tris, 1.0 mm, Mini Protein Gel (Thermo Fisher Scientific), and transferred to a polyvinylidene difluoride membrane using the iBlot 2 Dry Blotting System (Thermo Fisher Scientific). Specific protein bands were detected using anti-NRF2 (GTX103322, GeneTex, Irvine, CA, USA, 0.2 μg/mL) or anti-LAMIN B1 (GTX103292, GeneTex, 0.2 μg/mL) as primary antibodies, and HRP-conjugated anti-rabbit IgG (GTX213110-01, GeneTex, 0.02 μg/mL) as a secondary antibody using the iBind Automated Western System (Thermo Fisher Scientific). Protein bands were imaged using the FUSION-SOLO.7 S. EDGE V.070 (Vilber, France) and the SuperSignal™ West Femto Maximum Sensitivity Substrate (Thermo Fisher Scientific) as the chemiluminescent substrate and quantified using the ImageJ (ver. 1.53) [16].

Statistical analysis

All quantitative data are shown as the mean and standard deviation from three independent experiments. Tukey's or Dunnett's tests were performed using the R software (ver. 4.2.0) to compare the multiple groups.

Differential expression analysis was performed using the R software (ver. 4.2.0) and the DEseq2 (ver. 1.36.0) to calculate normalized counts, fold changes (FC), and adjusted p-values (p-adj). Differentially expressed genes (DEGs) were defined when $|\log_2(FC)| > 1$ and p-adj < 0.05. Hierarchical clustering was performed with $\log_2$-transformed normalized counts using the Python (ver. 3.9.4) with the SciPy (ver. 1.6.3). Gene ontology (GO) enrichment and gene set enrichment analyses (GSEA) were conducted using the Python package gseapy (ver. 0.10.5), and terms or gene sets with a false discovery rate (FDR) < 0.05 were shown as results. Hallmark gene sets [17] were used for GSEA. The DoRothEA R package (ver. 1.8.0) [18] was employed to estimate TFs using the VIPER algorithm [19].

Results

Effects of CAP on cell viability, IL6 expression, and RONS accumulation

The cell viability remained unaffected 24 h after CAP irradiation but declined after 48 h. Notably, cell viability decreased following 150 s of CAP irradiation at 72 h (Fig 1A). The number of
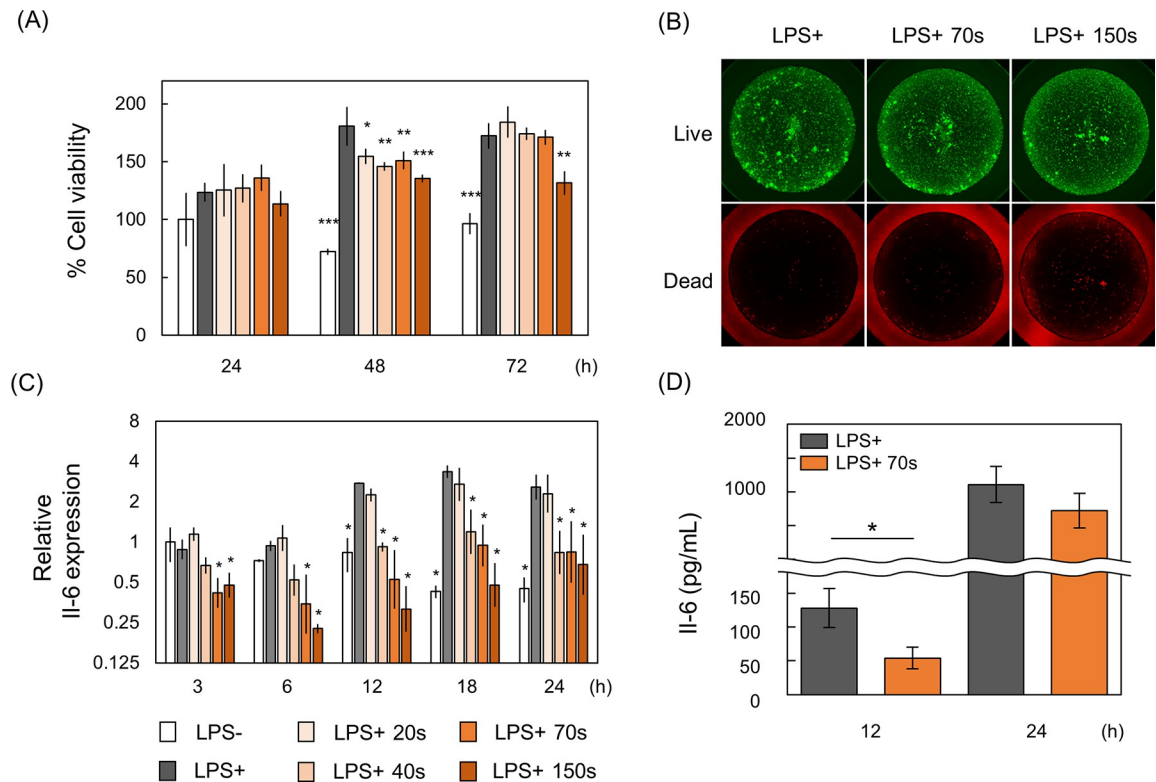
Fig 1. Cytotoxicity and IL6 expression following CAP irradiation. (A) Measurement of cell viability at 24–72 h post 20–150 s of CAP irradiation. Data represent the mean ± standard deviation of three independent experiments. *: $p < 0.05$, **: $p < 0.01$, ***: $p < 0.001$, compared to LPS+ using Dunnet's multiple comparison test. (B) Live/dead cell staining performed 24 h after CAP irradiation. (C) *IL6* expression measured by qRT-PCR at 3–24 h post CAP irradiation, normalized to LPS+ as the control. Data represent the mean ± standard deviation of three independent experiments. *: $p < 0.05$, compared to LPS+ using Dunnet's multiple comparison test. (D) Measurement of IL6 concentration in the culture medium using ELISA. *: $p < 0.05$, analyzed with Welch's t-test.

https://doi.org/10.1371/journal.pone.0292267.g001

dead cells showed no change after 70 s of CAP irradiation but slightly increased after 150 s (Fig 1B). *IL6* expression remained unaltered after 20 s of CAP irradiation; however, irradiation for 40 s or more significantly reduced expression levels at 12–24 h for 40 s of irradiation and at 3–24 h for 70 s and 150 s of irradiation (Fig 1C). CAP irradiation for 70 s led to a significant reduction in IL6 protein expression at 12 h (Fig 1D). These findings indicate that CAP irradiation exceeding 40 s exerts anti-inflammatory effects, while irradiation exceeding 150 s iscytotoxic. Thus, subsequent experiments utilized 70 s of CAP irradiation as it significantly suppressed IL6 expression without causing cytotoxic effects.

The accumulation of RONS in the cell culture medium due to CAP treatment was quantified using a colorimetric assay. This assay precisely measured the concentrations of the long-lived reactive species H_2O_2 and NO_2^-. In the absence of cells, CAP irradiation for 20–150 s resulted in the production of 14.9–65.0 μM H_2O_2 and 3.2–27.5 μM NO_2^-, both of which gradually degraded over time. However, when cells were present, H_2O_2 rapidly decomposed, while NO_2^- persisted even after 24 h (Fig 2).

RNA-Seq data analyses

To elucidate the anti-inflammatory mechanism of CAP, LPS-stimulated THP-1 cells were treated with and without CAP. RNA samples were extracted at 3, 6, 12, 18, and 24 h for RNA-Seq analysis. DEGs between the CAP-treated and the non-treated groups were analyzed. The
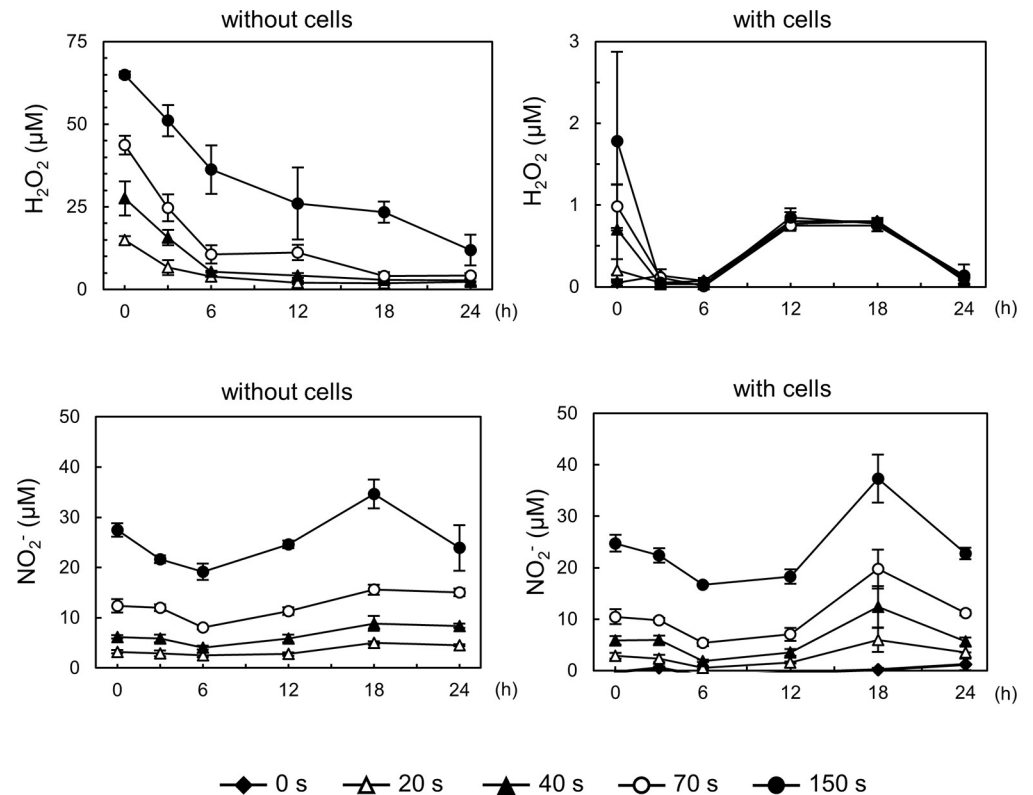
Fig 2. RONS accumulation in the CAP-irradiated medium. Concentrations of H_2O_2 and NO_2^- in the medium with or without cells after 0–24 h following CAP exposure for each irradiation time. Data are presented as the mean ± standard deviation of three independent experiments.

count of DEGs reached a maximum of 405 after 12 h, indicating that CAP irradiation altered gene expression patterns (Fig 3A and 3B).

Hierarchical clustering analysis was conducted using 740 genes identified as DEGs at any given time to assess significant alterations in gene expression patterns (Fig 4). These genes were categorized into five clusters: cluster 1 included 180 genes that were activated 12 h after CAP irradiation (late activated), cluster 2 included 198 genes that were primarily activated 3–12 h after CAP (early activated), cluster 3 included 214 genes that were inhibited after 12 h (late inhibited), cluster 4 included only four genes, and cluster 5 included 144 genes that were inhibited before 18 h (early inhibited).

GO enrichment analyses of each cluster showed that "positive regulation of inflammatory response" and other inflammation-related terms were significantly enriched in cluster 1 (Table 2). No GO terms were enriched in cluster 2. Inflammation-related GO terms such as "positive regulation of interferon-gamma production" and "antigen processing and presenta-tion of exogenous peptide antigen via MHC class II" were enriched in cluster 3. The major histocompatibility complex (MHC) class II-related genes were enriched in this cluster. Although cluster 1 showed a pro-inflammatory effect of CAP in the late phase, cluster 3 indi-cated that CAP simultaneously suppressed the inflammatory response. Cluster 5 also included inflammatory-related terms such as "positive regulation of cytokine production," "inflamma-tory response," "response to lipopolysaccharide," "positive regulation of interleukin-6 produc-tion," and "positive regulation of interleukin-1 beta production". Hence, CAP suppressed inflammation during the early phase.
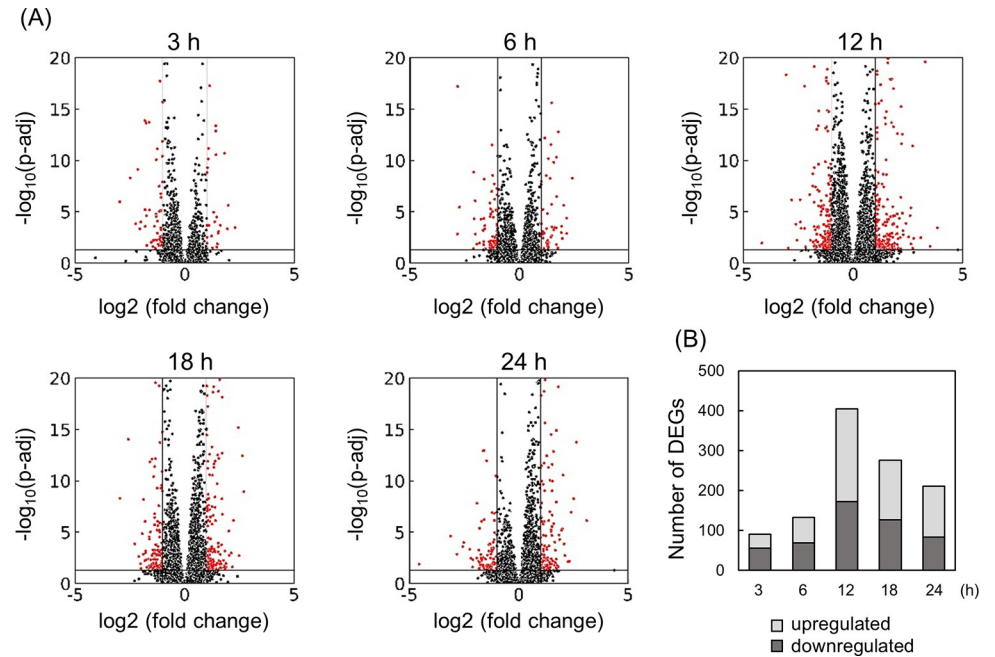
Fig 3. RNA-Seq analysis of THP-1 cells treated with CAP. (A) Volcano plot comparing the CAP-treated group with the non-treated group. Red points indicate DEGs, characterized by $|\log_2(FC)| > 1$ and p-adj < 0.05. (B) Stacked chart illustrating the numbers of upregulated (light grey) and downregulated (dark grey) DEGs.

https://doi.org/10.1371/journal.pone.0292267.g003

Fig 4. Hierarchical clustering of 740 DEGs at various time points. Input values consisted of log2-transformed normalized counts. The DEGs were classified into five clusters, comprising 180, 198, 214, 4, and 144 genes, respectively.

https://doi.org/10.1371/journal.pone.0292267.g004

Table 2. Notable GO terms of biological processes in each cluster.

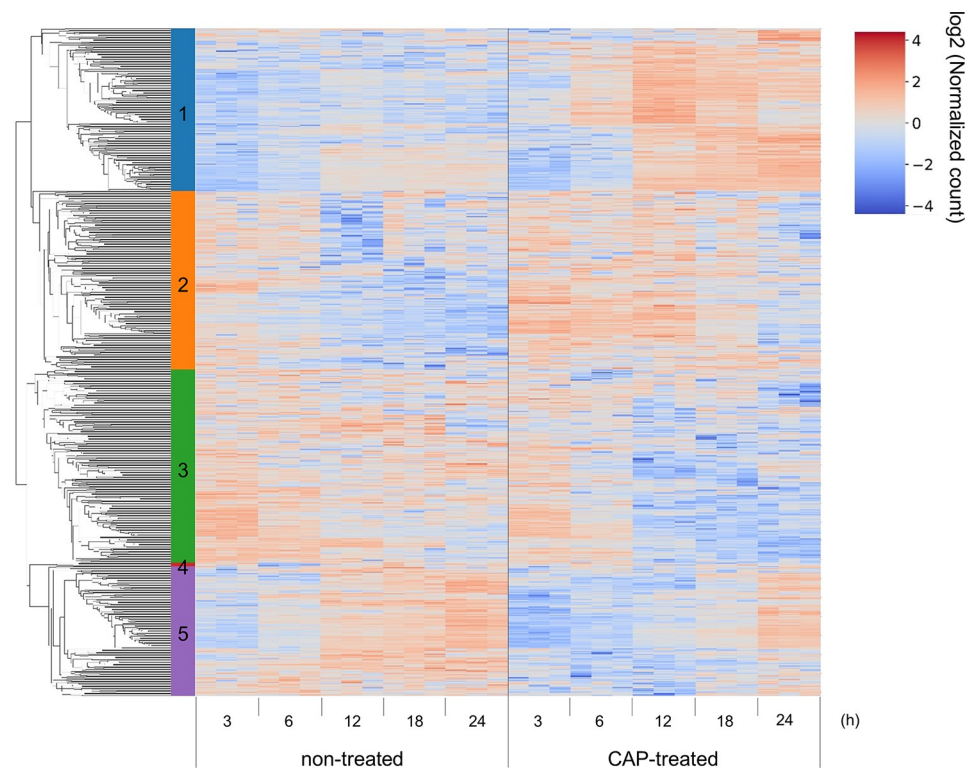| Cluster	Mode	GO Term (Biological Process)	Overlap	FDR	Genes
1	late activated	inflammatory response	12/230	0.0019	TMIGD3, MMP25, CXCL8, C5AR1, CHI3L1, ADM, CCL1, CDL4, FCGR2B, THBS1, S100A8, CMKLR1
		positive regulation of inflammatory response	6/89	0.0323	OSM, S100A12, CCL1, ETS1, PLA2G7, S100A8
3	late inhibited	positive regulation of interferon-gamma production	7/57	0.0031	IL23A, SLC11A1, HLA-DPB1, IL12B, PTPN22, IL18R1, HLA-DPA1
		antigen processing and presentation of exogenous peptide antigen via MHC class II	7/98	0.0126	HLA-DMA, HLA-DMB, HLA-DPB1, HLA-DRA, HLA-DQA1, HLA-DPA1, HLA-DQB1
		interleukin-23-mediated signaling pathway	3/9	0.0126	IL23A, STAT4, IL12B
5	early inhibited	positive regulation of cytokine production	13/335	0.0388	CD86, HHLA2, CD80, LILRB1, LILRB2, LILRA2, SCIMP, LILRA5, TLR1, FGFR, IL6, POLR3G, CCR7
		inflammatory response	11/230	0.0002	TLR1, IL6, PTGIR, CCL8, FPR1, CCL2, CCR7, SIGLEC1, FPR2, NLRC4, CXCL13
		response to lipopolysaccharide	9/159	0.0003	CD86, CX3CR1, IL6, CD80, CD180, CCL2, LILRB1, LILRB2, CXCL13
		positive regulation of interleukin-6 production	6/76	0.0010	TLR1, IL6, LILRB2, LILRA2, SCIMP, LILRA5
		positive regulation of interleukin-1 beta production	5/56	0.0024	IL6, MNDA, NLRC4, LILRA2, LILRA5

GSEA was conducted to examine the overall patterns of gene expression. The analysis revealed that the Normalized Enrichment Score (NES) for the "REACTIVE OXYGEN SPECIES PATHWAY" and "MTORC1 SIGNALING" gene sets were consistently elevated across all time points (Table 3). "TGF BETA SIGNALING" also showed significantly high NES values after 6 h. The NES values of "INFLAMMATORY RESPONSE" and "TNFA SIGNALING VIA NFKB" were significantly low at 3 h; however, they continued to increase at 6 h and beyond. These results not only confirm the anti-inflammatory effect of CAP but also suggest its pro-inflammatory effects after 12 h.

To identify the key TFs that regulate anti-inflammatory responses, TFs activated and inhibited by CAP were estimated using DoRothEA [18], and the average FDR at all time points was calculated for all TFs (Table 4). According to the results of the average FDR at 3–24 h, regulatory factor X5 (RFX5), which regulates MHC class II-related gene expression [20], was predicted to be the most repressed TF, whereas NRF2, which regulates defense mechanisms against oxidative stress via ARE [21], was predicted to be the most promoted TF. BTB and CNC homolog 1 (BACH1), which acts antagonistically with NRF2 [22], and NRF1, which acts like NRF2 via ARE [23], were also activated.

Table 3. Gene set enrichment analysis for each time point.

Gene Set		3 h	6 h	12 h	18 h	24 h	size
INFLAMMATORY RESPONSE	NES	-2.69	1.44	1.79	1.93	2.30	200
	FDR	0.000	0.056	0.009	0.001	0.000	
MTORC1 SIGNALING	NES	1.86	2.15	1.45	1.58	1.59	200
	FDR	0.004	0.003	0.036	0.015	0.009	
REACTIVE OXYGEN SPECIES PATHWAY	NES	1.95	2.81	2.39	2.28	2.28	49
	FDR	0.001	0.000	0.000	0.000	0.000	
TNFA SIGNALING VIA NFKB	NES	-2.57	2.11	2.23	2.27	2.23	200
	FDR	0.000	0.002	0.001	0.000	0.000	
TGF BETA SIGNALING	NES	1.27	1.87	2.02	2.26	2.12	54
	FDR	0.154	0.007	0.005	0.000	0.000	

Table 4. Top five estimated TFs activated or inhibited by CAP.

TF	3 h		6 h		12 h		18 h		24 h		FDR mean
	t value	FDR	t value	FDR	t value	FDR	t value	FDR	t value	FDR	
RFX5	-3.982	0.211	-9.903	0.040	-81.048	0.000	-8.116	0.145	-4.417	0.203	0.120
NRF2	6.752	0.118	12.425	0.033	10.256	0.069	5.125	0.194	4.640	0.203	0.123
BACH1	4.029	0.211	15.641	0.026	3.856	0.260	3.487	0.199	2.984	0.267	0.193
NRF1	3.131	0.272	3.558	0.216	4.278	0.233	6.321	0.145	2.949	0.267	0.227
JUNB	3.868	0.222	1.900	0.364	3.225	0.290	4.402	0.194	2.794	0.267	0.267

https://doi.org/10.1371/journal.pone.0292267.t004

Protein level alteration of the CAP-induced TFs

Since NRF2 was estimated to be the most activated TF following CAP irradiation, the nuclear transition of NRF2 was measured using western blotting. A significant increase of NRF2 accumulation in the nucleus of CAP-irradiated THP-1 cells was confirmed, suggesting that the nuclear transition of NRF2 was promoted by CAP irradiation (Fig 5).

Discussion

Plasma medicine has emerged as a promising field of research for the treatment of various medical conditions, with a particular focus on wound healing and sterilization. Some studies have suggested the anti-inflammatory effects of CAP [5,9,10] and its application in the dental field, such as in periodontal disease [6]; however, how CAP inhibits inflammatory responses remains unclear. In the present study, we identified and confirmed the key TFs using transcriptome analysis to elucidate the anti-inflammatory mechanisms of CAP. THP-1, a human acute monocytic leukemia cell line, was used in the present study because monocytes play a central role in periodontal diseases, such as initiating inflammation upon contact with pathogens, inflammatory cytokine production, and T cell activation [24]. To induce inflammatory condition, Pg-derived LPS was employed since Pg is one of the most important pathogens in periodontitis [25,26], and Pg-LPS has been reported to induce inflammation in THP-1 [27,28].
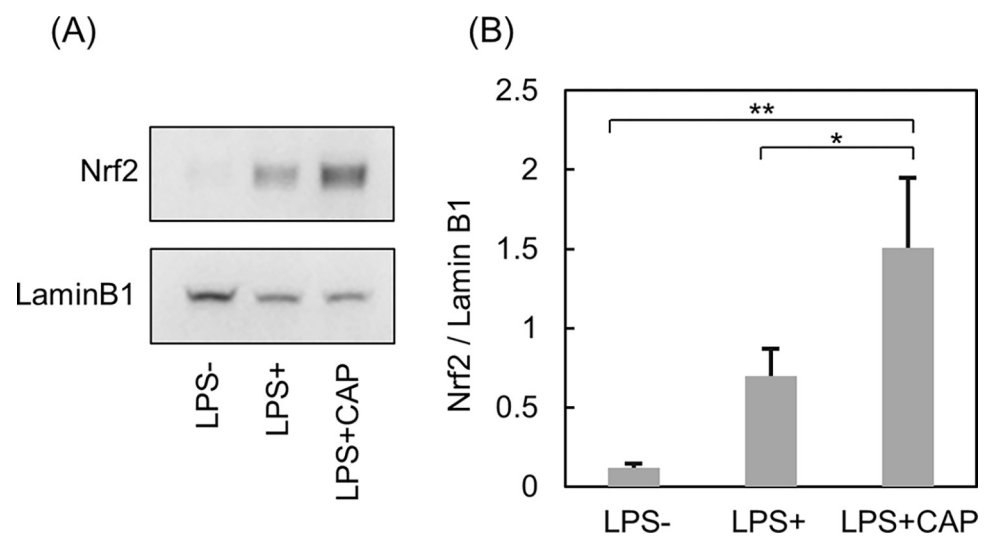

Fig 5. NRF2 localization in the nucleus of THP-1 cells. Western blotting images (A) and normalized quantification (B).LAMIN B1 was used as loading control. Data are presented as the mean ± standard deviation of three independent experiments. *p <0.05, **p <0.01; Tukey's multiple comparison test was performed.

https://doi.org/10.1371/journal.pone.0292267.g005

Pg-derived LPS is known to induce inflammation mainly via TLR2 [29], and THP-1 expresses TLR2 more than TLR4 [30]. Proteins present in serum, such as LPS-binding protein, have a critical role in inducing interferon (IFN)-related genes [31], and IFN signaling is important in inflammasome activation against infection [32]. Thus, THP-1 was stimulated with Pg-LPS in an FBS-supplemented medium to mimic the *in vivo* environment.

CAP irradiation exhibited a dose-dependent suppression of *IL6* expression and increased cytotoxicity. The quantity of RONS generated at each dose was quantified. Non-irradiated cells did not produce H_2O_2 or NO_2^- (Fig 2), indicating that the RONS were produced by the reaction between CAP and atmosphere and medium. H_2O_2 in the medium without cells was gradually degraded after 24 h. In contrast, H_2O_2 rapidly degraded in the medium with cells, indicating that THP-1 cells have a high capacity to decompose it. However, the NO_2^- concentration was maintained for 24 h after irradiation, regardless of the presence or absence of cells. The anti-inflammatory effects of CAP are presumably attributed to NO_2^- and its reduced form, nitric oxide, which regulates inflammation [33–35].

GO enrichment analysis revealed that CAP inhibited MHC class II-related gene and *IL23* expression. MHC class II, expressed on the membrane of antigen-presenting cells (APCs), such as monocytes, dendritic cells, and macrophages, mediates the presentation of exogenous antigens to CD4+ naïve T cells and promotes helper T cell differentiation [36,37]. CD4+ naïve T cells stimulated by APCs differentiate into subsets of helper T cells: Th1, which eliminates intracellular pathogens; Th2, which controls the immune response against extracellular parasites; Th17, which is responsible for mounting the immune response against extracellular bacteria and fungi; and regulatory T cells (Treg), which negatively regulates inflammation [37]. The involvement of Th1, Th2, and Th17 cells at periodontal disease sites has also been observed [38,39]. CD4+ naïve T cells differentiate into Th17 cells upon stimulation with IL6 and IL23 [40]. Th17 secretes IL17, which induces inflammation in other cells, such as fibroblasts and macrophages, and proliferates in the presence of IL23 [41,42]. IL17 is overexpressed in tissues with chronic inflammation, including in periodontitis, and the IL23 antagonist inhibits the *IL17* expression and inflammation [42,43]. Following CAP irradiation, our results revealed the inhibition of MHC class II-related genes, IL6 and *IL23*, suggesting that CAP attenuates Th17 cell differentiation and proliferation, leading to anti-inflammatory effects.

GSEA revealed that CAP activated transforming growth factor β (TGF-β) and mTORC1 signaling. TGF-β acts on CD4+ naïve T cells to inhibit the differentiation into Th1 and Th2 and promote differentiation into Tregs [44]. TGF-β also promotes CD4+ naïve T cell differentiation into Th17 with IL6 [37]; however, IL6 was downregulated by CAP, suggesting that CAP irradiation biases helper T cell population toward the Treg subset. Since pro-inflammatory effects have been observed by inhibiting mTORC1 [45,46], activating mTORC1 signaling using CAP may reduce inflammatory responses.

In the present study, NRF2 was the most upregulated TF, and its nuclear translocation was confirmed by western blotting. NRF2 activation via CAP was consistent with previous studies [13,14,47]. Under normal, non-stressful conditions, NRF2 undergoes ubiquitination by Kelch-like ECH-associated protein 1 (KEAP1) and subsequent proteasomal degradation. However, during oxidative stress, KEAP1 undergoes oxidation, leading to the release of NRF2. This release further enhances the expression of antioxidant genes regulated by AREs [21]. One such antioxidant gene is heme oxygenase 1 (*HO-1*), which generates the anti-inflammatory molecules carbon monoxide and biliverdin as byproducts of heme decomposition [48]. Additionally, NRF2 binds directly to regions proximal to the *IL6* and *IL1β* genes, inhibiting their expression [49]. Furthermore, activation of NRF2 inhibits the nuclear factor-kappa B pathway and ameliorates periodontitis in a rat model [50]. Furthermore, inhibition of IL6 and NRF2 nuclear translocation was confirmed in this study. Thus, NRF2 plays a pivotal role in
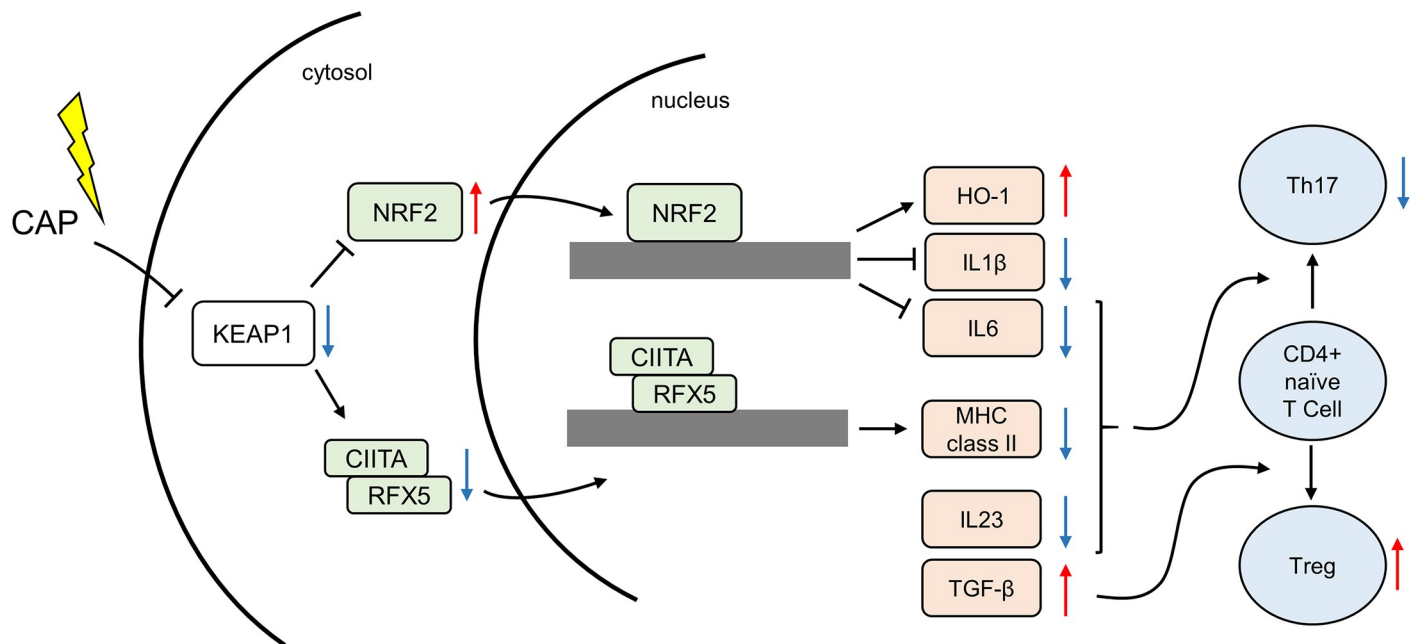
Fig 6. Schematic illustration depicting the proposed anti-inflammatory mechanism of CAP. Red and blue arrows represent the CAP-induced activation and suppression, respectively, in each pathway. CAP: Cold atmospheric plasma; KEAP1: Kelch-like ECH-associated protein 1; NRF2: Nuclear factor erythroid 2-related factor 2; CIITA: Class II transactivator; RFX5: Regulatory factor X5; HO-1: Heme oxygenase 1; IL1β: Interleukin 1β; IL6: Interleukin 6; MHC class II: Major histocompatibility complex class II; IL23: Interleukin 23; TGF-β: Transforming growth factor β; Treg: Regulatory T cell.

suppressing inflammatory responses by activating antioxidant genes and inhibiting inflammatory cytokines.

In contrast, RFX5 was estimated to be the most downregulated TF. RFX5 binds to class II transactivator (CIITA) and other proteins and positively regulates MHC class II genes [51]. KEAP1 oxidation downregulates CIITA activity [52], suggesting that CAP suppresses MHC class II gene expression by affecting KEAP1 and CIITA. CAP treatment appeared to activate BACH1 and NRF1. BACH1 binds to AREs and competes with NRF2 for interaction [22]. BACH1 activation contributes to homeostasis-like effects by suppressing the NRF2 pathway. NRF1 overlaps with NRF2 [23], suggesting that it has anti-inflammatory and antioxidant effects.

However, the study had several limitations: the cell type was limited to monocytes, and no *in vivo* studies were conducted. Although NRF2 activation and nuclear transition promoted by CAP have been confirmed, KEAP1 oxidation induced by CAP and the KEAP1-CIITA pathway needs to be elucidated. Therefore, further research is necessary to reveal the inhibition of CD4 + naïve T cell differentiation into Th17 cell by CAP.

Collectively, our findings demonstrated that the NRF2 pathway is involved in mediating the anti-inflammatory effects of CAP, potentially by suppressing pro-inflammatory genes, such as *IL6*, and upregulating anti-inflammatory genes, such as *HO-1*. Additionally, CAP downregulated RFX5, a regulator of MHC class II expression, and *IL23* while promoting TGF-β signaling. These findings suggest that CAP attenuated Th17 cell activity and promoted Treg cell differentiation, thus contributing to its anti-inflammatory effects (Fig 6).

Supporting information

S1 Raw images.
(PDF)

Acknowledgments

Author Contributions

Conceptualization: Ito Hirasawa, Takaya Oshita, Akiko Togi.

Data curation: Ito Hirasawa, Haruka Odagiri, Giri Park, Rutvi Sanghavi, Katsunori Yoshikawa.

Formal analysis: Ito Hirasawa, Haruka Odagiri, Giri Park, Rutvi Sanghavi.

Investigation: Ito Hirasawa, Haruka Odagiri, Giri Park, Rutvi Sanghavi.

Methodology: Ito Hirasawa, Haruka Odagiri, Giri Park, Rutvi Sanghavi, Katsunori Yoshikawa, Koji Mizutani, Yasuo Takeuchi, Hiroaki Kobayashi, Sayaka Katagiri, Takanori Iwata, Akira Aoki.

Resources: Takaya Oshita.

Supervision: Akiko Togi, Katsunori Yoshikawa, Koji Mizutani, Yasuo Takeuchi, Hiroaki Kobayashi, Sayaka Katagiri, Takanori Iwata, Akira Aoki.

Validation: Ito Hirasawa, Katsunori Yoshikawa.

Visualization: Ito Hirasawa.

Writing – original draft: Ito Hirasawa.

Writing – review & editing: Akira Aoki.

References

1. von Woedtke T, Reuter S, Masur K, Weltmann KD. Plasmas for medicine. Phys Rep. 2013; 530: 291–320. https://doi.org/10.1016/j.physrep.2013.05.005

2. Fridman G, Friedman G, Gutsol A, Shekhter AB, Vasilets VN, Fridman A. Applied plasma medicine. Plasma Process Polym. 2008; 5: 503–533. https://doi.org/10.1002/ppap.200700154

3. Laroussi M. Plasma medicine: A brief Introduction. Plasma. 2018; 1: 47–60. https://doi.org/10.3390/plasma1010005

4. Papapanou PN, Sanz M, Buduneli N, Dietrich T, Feres M, Fine DH, et al. Periodontitis: consensus report of workgroup 2 of the 2017 World Workshop on the Classification of Periodontal and Peri-Implant Diseases and Conditions. J Clin Periodontol. 2018; 45 Suppl 20: S162–S170. https://doi.org/10.1111/jcpe.12946 PMID: 29926490

5. Zhang Y, Xiong Y, Xie P, Ao X, Zheng Z, Dong X, et al. Non-thermal plasma reduces periodontitis-induced alveolar bone loss in rats. Biochem Biophys Res Commun. 2018; 503: 2040–2046. https://doi.org/10.1016/j.bbrc.2018.07.154 PMID: 30086885

6. Küçük D, Savran L, Ercan UK, Yarali ZB, Karaman O, Kantarci A, et al. Evaluation of efficacy of non-thermal atmospheric pressure plasma in treatment of periodontitis: a randomized controlled clinical trial. Clin Oral Investig. 2020; 24: 3133–3145. https://doi.org/10.1007/s00784-019-03187-2 PMID: 31897708

7. López M, Calvo T, Prieto M, Múgica-Vidal R, Muro-Fraguas I, Alba-Elías F, et al. A review on non-thermal atmospheric plasma for food preservation: Mode of action, determinants of effectiveness, and applications. Front Microbiol. 2019; 10: 622. https://doi.org/10.3389/fmicb.2019.00622 PMID: 31001215

8. Yost AD, Joshi SG. Atmospheric nonthermal plasma-treated PBS inactivates Escherichia coli by oxidative DNA damage. PLoS One. 2015; 10: e0139903. https://doi.org/10.1371/journal.pone.0139903 PMID: 26461113

9. Bekeschus S, Schmidt A, Jablonowski H, Bethge L, Hasse S, Wende K, et al. Environmental control of an argon plasma effluent and Its role in THP-1 monocyte function. IEEE Trans Plasma Sci. 2017; 45: 3336–3341. https://doi.org/10.1109/TPS.2017.2771740

10. Hasse S, Hahn O, Kindler S, von Woedtke T, Metelmann H-R, Masur K. Atmospheric pressure plasma jet application on human oral mucosa modulates tissue regeneration. Plasma Med. 2014; 4: 117–129. https://doi.org/10.1615/plasmamed.2014011978

11. Barton A, Wende K, Bundscherer L, Hasse S, Schmidt A, Bekeschus S, et al. Nonthermal plasma increases expression of wound healing related genes in a keratinocyte cell line. Plasma Med. 2013; 3: 125–136. https://doi.org/10.1615/plasmamed.2014008540

12. Bekeschus S, Meyer D, Arlt K, von Woedtke T, Miebach L, Freund E, et al. Argon plasma exposure zugments costimulatory ligands and cytokine release in human monocyte-derived dendritic cells. Int J Mol Sci. 2021; 22. https://doi.org/10.3390/ijms22073790 PMID: 33917526

13. Schmidt A, von Woedtke T, Vollmar B, Hasse S, Bekeschus S. Nrf2 signaling and inflammation are key events in physical plasma-spurred wound healing. Theranostics. 2019; 9: 1066–1084. https://doi.org/10.7150/thno.29754 PMID: 30867816

14. Schmidt A, Dietrich S, Steuer A, Weltmann KD, von Woedtke T, Masur K, et al. Non-thermal plasma activates human keratinocytes by stimulation of antioxidant and phase II pathways. J Biol Chem. 2015; 290: 6731–6750. https://doi.org/10.1074/jbc.M114.603555 PMID: 25589789

15. Livak KJ, Schmittgen TD. Analysis of relative gene expression data using real-time quantitative PCR and the 2− ΔΔCT method. Methods. 2001; 25: 402–408. https://doi.org/10.1006/meth.2001.1262 PMID: 11846609

16. Schneider CA, Rasband WS, Eliceiri KW. NIH Image to ImageJ: 25 years of image analysis. Nat Methods. 2012; 9: 671–675. https://doi.org/10.1038/nmeth.2089 PMID: 22930834

17. Liberzon A, Birger C, Thorvaldsdóttir H, Ghandi M, Mesirov JP, Tamayo P. The Molecular Signatures Database (MSigDB) hallmark gene set collection. Cell Syst. 2015; 1: 417–425. https://doi.org/10.1016/j.cels.2015.12.004 PMID: 26771021

18. Garcia-Alonso L, Holland CH, Ibrahim MM, Turei D, Saez-Rodriguez J. Benchmark and integration of resources for the estimation of human transcription factor activities. Genome Res. 08/2019; 29: 1363–1375. https://doi.org/10.1101/gr.240663.118 PMID: 31340985

19. Alvarez MJ, Shen Y, Giorgi FM, Lachmann A, Ding BB, Ye BH, et al. Functional characterization of somatic mutations in cancer using network-based inference of protein activity. Nat Genet. 8/2016; 48: 838–847. https://doi.org/10.1038/ng.3593 PMID: 27322546

20. Aftab S, Semenec L, Chu JS-C, Chen N. Identification and characterization of novel human tissue-specific RFX transcription factors. BMC Evol Biol. 2008; 8: 226. https://doi.org/10.1186/1471-2148-8-226 PMID: 18673564

21. Tonelli C, Chio IIC, Tuveson DA. Transcriptional Regulation by Nrf2. Antioxid Redox Signal. 2018; 29: 1727–1745. https://doi.org/10.1089/ars.2017.7342 PMID: 28899199

22. Zhang X, Guo J, Wei X, Niu C, Jia M, Li Q, et al. Bach1: function, regulation, and involvement in disease. Oxid Med Cell Longev. 2018; 2018: 1347969. https://doi.org/10.1155/2018/1347969 PMID: 30370001

23. Kim HM, Han JW, Chan JY. Nuclear factor erythroid-2 like 1 (NFE2L1): Structure, function and regulation. Gene. 2016; 584: 17–25. https://doi.org/10.1016/j.gene.2016.03.002 PMID: 26947393

24. Liu YZ, Maney P, Puri J, Zhou Y, Baddoo M, Strong M, et al. RNA-sequencing study of peripheral blood monocytes in chronic periodontitis. Gene. 2016; 581: 152–160. https://doi.org/10.1016/j.gene.2016.01.036 PMID: 26812355

25. Socransky SS, Haffajee AD, Cugini MA, Smith C, Kent RL Jr. Microbial complexes in subgingival plaque. J Clin Periodontol. 1998; 25: 134–144. https://doi.org/10.1111/j.1600-051x.1998.tb02419.x PMID: 9495612

26. Jain S, Darveau RP. Contribution of Porphyromonas gingivalis lipopolysaccharide to periodontitis. Periodontol 2000. 2010; 54: 53–70. https://doi.org/10.1111/j.1600-0757.2009.00333.x PMID: 20712633

27. Gokyu M, Kobayashi H, Nanbara H, Sudo T, Ikeda Y, Suda T, et al. Thrombospondin-1 production is enhanced by Porphyromonas gingivalis lipopolysaccharide in THP-1 cells. PLoS One. 2014; 9: e115107. https://doi.org/10.1371/journal.pone.0115107 PMID: 25501558

28. Zhu X-Q, Lu W, Chen Y, Cheng X-F, Qiu J-Y, Xu Y, et al. Effects of Porphyromonas gingivalis lipopolysaccharidetolerized monocytes on inflammatory responses in neutrophils. PLoS One. 2016; 11: e0161482. https://doi.org/10.1371/journal.pone.0161482 PMID: 27536946

29. Zhang D, Chen L, Li S, Gu Z, Yan J. Lipopolysaccharide (LPS) of Porphyromonas gingivalis induces IL-1β, TNF-α and IL-6 production by THP-1 cells in a way different from that of Escherichia coli LPS. Innate Immun. 2008; 14: 99–107. https://doi.org/10.1177/1753425907088244 PMID: 18713726

30. Zhang FX, Kirschning CJ, Mancinelli R, Xu X-P, Jin Y, Faure E, et al. Bacterial lipopolysaccharide activates nuclear factor-κB through interleukin-1 signaling mediators in cultured human dermal endothelial cells and mononuclear phagocytes*. J Biol Chem. 1999; 274: 7611–7614. https://doi.org/10.1074/jbc.274.12.7611 PMID: 10075645

31. Kato A, Ogasawara T, Homma T, Saito H, Matsumoto K. Lipopolysaccharide-binding protein critically regulates lipopolysaccharide-induced IFN-beta signaling pathway in human monocytes. J Immunol. 2004; 172: 6185–6194. https://doi.org/10.4049/jimmunol.172.10.6185 PMID: 15128806

32. Aral K, Milward MR, Kapila Y, Berdeli A, Cooper PR. Inflammasomes and their regulation in periodontal disease: A review. J Periodontal Res. 2020; 55: 473–487. https://doi.org/10.1111/jre.12733 PMID: 31960443

33. Waltz P, Escobar D, Botero AM, Zuckerbraun BS. Nitrate/Nitrite as Critical Mediators to Limit Oxidative Injury and Inflammation. Antioxid Redox Signal. 2015; 23: 328–339. https://doi.org/10.1089/ars.2015. 6256 PMID: 26140517

34. Zhan J, Nakao A, Sugimoto R, Dhupar R, Wang Y, Wang Z, et al. Orally administered nitrite attenuates cardiac allograft rejection in rats. Surgery. 2009; 146: 155–165. https://doi.org/10.1016/j.surg.2009.05. 002 PMID: 19628069

35. Ohtake K, Koga M, Uchida H, Sonoda K, Ito J, Uchida M, et al. Oral nitrite ameliorates dextran sulfate sodium-induced acute experimental colitis in mice. Nitric Oxide. 2010; 23: 65–73. https://doi.org/10. 1016/j.niox.2010.04.004 PMID: 20399279

36. Rock KL, Reits E, Neefjes J. Present yourself! by MHC class I and MHC class II molecules. Trends Immunol. 2016; 37: 724–737. https://doi.org/10.1016/j.it.2016.08.010 PMID: 27614798

37. Luckheeram RV, Zhou R, Verma AD, Xia B. CD4+T cells: Differentiation and functions. Clin Dev Immunol. 2012; 2012. https://doi.org/10.1155/2012/925135 PMID: 22474485

38. Campbell L, Millhouse E, Malcolm J, Culshaw S. T cells, teeth and tissue destruction—what do T cells do in periodontal disease? Mol Oral Microbiol. 2016; 31: 445–456. https://doi.org/10.1111/omi.12144 PMID: 26505640

39. Berglundh T, Liljenberg B, Lindhe J. Some cytokine profiles of T-helper cells in lesions of advanced periodontitis. J Clin Periodontol. 2002; 29: 705–709. https://doi.org/10.1034/j.1600-051x.2002.290807.x PMID: 12390567

40. Cerboni S, Gehrmann U, Preite S, Mitra S. Cytokine-regulated Th17 plasticity in human health and diseases. Immunology. 2021; 163: 3–18. https://doi.org/10.1111/imm.13280 PMID: 33064842

41. Toussirot E. The IL23/Th17 pathway as a therapeutic target in chronic inflammatory diseases. Inflamm Allergy Drug Targets. 2012; 11: 159–168. https://doi.org/10.2174/187152812800392805 PMID: 22280236

42. Bunte K, Beikler T. Th17 cells and the IL-23/IL-17 axis in the pathogenesis of periodontitis and immune-mediated inflammatory diseases. Int J Mol Sci. 2019; 20: 3394. https://doi.org/10.3390/ijms20143394 PMID: 31295952

43. Azman R, Lappin DF, MacPherson A, Riggio M, Robertson D, Hodge P, et al. Clinical associations between IL-17 family cytokines and periodontitis and potential differential roles for IL-17A and IL-17E in periodontal immunity. Inflamm Res. 2014; 63: 1001–1012. https://doi.org/10.1007/s00011-014-0776-7 PMID: 25369802

44. Yoshimura A, Wakabayashi Y, Mori T. Cellular and molecular basis for the regulation of inflammation by TGF-beta. J Biochem. 2010; 147: 781–792. https://doi.org/10.1093/jb/mvq043 PMID: 20410014

45. Collins SL, Oh MH, Sun IH, Chan-Li Y, Zhao L, Powell JD, et al. mTORC1 signaling regulates proinflammatory macrophage function and metabolism. J Immunol. 2021; 207: 913–922. https://doi.org/10.4049/ jimmunol.2100230 PMID: 34290107

46. Weichhart T, Costantino G, Poglitsch M, Rosner M, Zeyda M, Stuhlmeier KM, et al. The TSC-mTOR signaling pathway regulates the innate inflammatory response. Immunity. 2008; 29: 565–577. https:// doi.org/10.1016/j.immuni.2008.08.012 PMID: 18848473

47. Scharf C, Eymann C, Emicke P, Bernhardt J, Wilhelm M, Görries F, et al. Improved wound healing of airway epithelial cells is mediated by cold atmospheric plasma: a time course-related proteome analysis. Oxid Med Cell Longev. 2019; 2019: 7071536. https://doi.org/10.1155/2019/7071536 PMID: 31223425

48. Pae HO, Chung HT. Heme oxygenase-1: its therapeutic roles in inflammatory diseases. Immune Netw. 2009; 9: 12–19. https://doi.org/10.4110/in.2009.9.1.12 PMID: 20107533

49. Kobayashi EH, Suzuki T, Funayama R, Nagashima T, Hayashi M, Sekine H, et al. Nrf2 suppresses macrophage inflammatory response by blocking proinflammatory cytokine transcription. Nat Commun. 2016; 7: 11624. https://doi.org/10.1038/ncomms11624 PMID: 27211851

50. Tian Y, Li Y, Liu J, Lin Y, Jiao J, Chen B, et al. Photothermal therapy with regulated Nrf2/NF-κB signaling pathway for treating bacteria-induced periodontitis. Bioact Mater. 2022; 9: 428–445. https://doi.org/10. 1016/j.bioactmat.2021.07.033 PMID: 34820581

51. LeibundGut-Landmann S, Waldburger JM, Krawczyk M, Otten LA, Suter T, Fontana A, et al. Mini-review: Specificity and expression of CIITA, the master regulator of MHC class II genes. Eur J Immunol. 2004; 34: 1513–1525. https://doi.org/10.1002/eji.200424964 PMID: 15162420

52. Wijdeven RH, van Luijn MM, Wierenga-Wolf AF, Akkermans JJ, van den Elsen PJ, Hintzen RQ, et al. Chemical and genetic control of IFNγ-induced MHCII expression. EMBO Rep. 2018;19. https://doi.org/10.15252/embr.201745553 PMID: 30021835